tvst

Retina

Investigating the Spatiotemporal Summation of Perimetric Stimuli in Dry Age-Related Macular Degeneration

Aoife M. L. Hunter[1], Roger S. Anderson[1,2], Tony Redmond[3], David F. Garway-Heath[2], and Pádraig J. Mulholland[1–3]

[1] Centre for Optometry and Vision Science, Biomedical Sciences Research Institute, Ulster University, Coleraine, UK
[2] National Institute for Health Research Moorfields Biomedical Research Centre, Moorfields Eye Hospital NHS Foundation Trust and UCL Institute of Ophthalmology, London, UK
[3] School of Optometry and Vision Sciences, Cardiff University, Cardiff, UK

Correspondence: Aoife M. L. Hunter, Centre for Optometry and Vision Science, Biomedical Sciences Research Institute, Ulster University, Cromore Road, Coleraine, UK BT52 1SA, UK. e-mail: a.hunter@ulster.ac.uk

Received: March 29, 2023
Accepted: September 26, 2023
Published: November 29, 2023

Keywords: spatial summation; temporal summation; age-related macular degeneration; microperimetry; perimetry; ricco's area

Citation: Hunter AML, Anderson RS, Redmond T, Garway-Heath DF, Mulholland PJ. Investigating the spatiotemporal summation of perimetric stimuli in dry age-related macular degeneration. Transl Vis Sci Technol. 2023;12(11):37, https://doi.org/10.1167/tvst.12.11.37

Purpose: To measure achromatic spatial, temporal, and spatiotemporal summation in dry age-related macular degeneration (AMD) compared to healthy controls under conditions of photopic gaze-contingent perimetry.

Methods: Twenty participants with dry AMD (mean age, 74.6 years) and 20 healthy controls (mean age, 67.8 years) performed custom, gaze-contingent perimetry tests. An area-modulation test generated localized estimates of Ricco's area (RA) at 2.5° and 5° eccentricities along the 0°, 90°, 180°, and 270° meridians. Contrast thresholds were measured at the same test locations for stimuli of six durations (3.7–190.4 ms) with a Goldmann III stimulus (GIII, 0.43°) and RA-scaled stimuli. The upper limit (critical duration) of complete temporal summation (using the GIII stimulus) and spatiotemporal summation (using the RA stimuli) was estimated using iterative two-phase regression analysis.

Results: Median (interquartile range [IQR]) RA estimates were significantly larger in AMD participants (2.5°: 0.21 [0.09–0.41] deg^2; 5°: 0.32 [0.15–0.65 deg^2]) compared to healthy controls (2.5°: 0.08 [0.05–0.13] deg^2; 5°: 0.15 [0.08–0.22] deg^2) at all test locations (all $P < 0.05$). No significant difference in median critical duration was found in AMD participants with the GIII stimulus (19.6 [9.9–30.4] ms) and RA-scaled stimuli (22.9 [13.9–40.3] ms) compared to healthy controls (GIII: 17.0 [11.3–24.0] ms; RA-scaled: 22.4 [14.3–33.1] ms) at all test locations (all $P > 0.05$).

Conclusions: Spatial summation is altered in dry AMD, without commensurate changes in temporal summation.

Translational Relevance: The sensitivity of perimetry to AMD may be improved by utilizing stimuli that probe alterations in spatial summation in the disease.

Introduction

Age-related macular degeneration (AMD) is one of the leading causes of sight loss worldwide.[1] In the United Kingdom alone, approximately 0.5 million people are visually impaired due to the condition, with an estimated rise to 1.23 million by 2050.[2] The two phenotypically distinct forms of the disease are wet (neovascular) and dry (atrophic) AMD. Anti–vascular endothelial growth factor intravitreal injections are primarily used to treat the wet form of this progressive condition.[3–5] There is currently no validated therapy for dry AMD. Novel interventions for the treatment of dry AMD are therefore the primary focus of numerous clinical trials.[6–9]

The measurement of visual function is central to the clinical investigation and management of AMD and as an endpoint in trials investigating novel therapeutic interventions. Currently, high-contrast visual acuity serves as the primary functional biomarker for disease detection and monitoring.[10–13] Although simple to undertake and familiar to patients, this test reflects only visual function within a limited region

of the visual field (fovea or preferred retinal locus [PRL]). Also, any changes are potentially non-specific to the AMD disease process. Visual acuity may also be spared depending on the location, extent, and form of AMD-associated lesions,[14] with the result that these measures are only weakly related to quality of life in the disease.[15–17] In view of such limitations, microperimetry (also known as fundus perimetry,[18,19] fundus-controlled perimetry,[20] or fundus-related perimetry[21,22]) undertaken in photopic,[23,24] mesopic,[25–30] and scotopic[28,30,31] conditions has increasingly gained acceptance as a mainstream clinical test of visual function in AMD.[32–36] This test permits the measurement of achromatic and/or chromatic contrast thresholds at multiple, pre-selected locations across the central visual field, using a stimulus of constant area (typically Goldmann III [GIII], 0.43°) and presentation duration (100–200 ms). To account for voluntary and involuntary eye movements, stimulus position is adjusted in real time. The ability to present stimuli to the same retinal location enables more accurate colocalization and comparison with colocalized measures of retinal structure, particularly in individuals with unstable fixation.[22,37]

Although widely adopted, microperimetry suffers from a number of significant limitations, including high measurement variability,[37] a limited dynamic range,[37,38] and a poor sensitivity to the effects of early and intermediate AMD.[39] Although test sensitivity and dynamic range may be improved by reducing the adapting luminance of the test to mesopic[40,41] or scotopic[29,42] levels, the stimuli used in all forms of the test were not selected with any reference to how the visual system integrates light energy over space (spatial summation) or time (temporal summation) and whether these processes are altered in AMD. Rather, stimuli were selected to be the same as those used in standard automated perimetry and earlier kinetic perimetry[43] (i.e., Goldmann areas I–IV and presentation duration 100–200 ms to be shorter than the assumed minimum velocity of voluntary saccadic eye movements).

Ricco's law[44] states that the product of stimulus contrast (ΔI) and area (A) is constant at threshold ($\Delta I \times A = k$). This relationship holds true for a range of small-area stimuli. The largest stimulus for which Ricco's law holds is known as Ricco's area. For larger stimuli, Ricco's law breaks down and only partial summation occurs. Ricco's area is known to enlarge with reduced background luminance,[45,46] with increasing visual field eccentricity,[47–50] and in various conditions, including glaucoma,[51,52] amblyopia,[53] retinitis pigmentosa,[54] and myopia.[55] Such changes in spatial summation are thought to reflect a noise-compensatory mechanism whereby the visual system seeks to maximize visual sensitivity for given environmental conditions or where cellular density and/or function are altered. Importantly, it has been found that perimetric stimuli designed to map localized changes in spatial summation in glaucoma offer a more favorable test sensitivity to measurement variability (disease signal/noise ratio) than that of the standard luminance-modulated achromatic GIII stimulus.[52,56]

In a similar manner to spatial summation, light energy is also summed over time (temporal summation). This process is governed by Bloch's law.[57] Analogous to Ricco's law, in this case the product of stimulus contrast (ΔI) at threshold and stimulus duration (t) are constant ($\Delta I \times t = k$). The maximum stimulus duration for which complete temporal summation occurs is referred to as the critical duration. Beyond this point, incomplete temporal summation is observed. Similar to the spatial domain, temporal summation varies with background luminance[58] and stimulus area,[46,59,60] as well as in some forms of ocular disease. Mulholland et al.[51] reported a longer critical duration in patients with early glaucoma compared to healthy controls and hypothesized that this is a result of retinal ganglion cell (RGC) death, premorbid RGC dysfunction, and/or changes in the receptive field properties of cells in the visual cortex. Interestingly, they found this change in temporal summation in glaucoma when both a GIII stimulus (likely exhibiting incomplete spatial summation) and a Ricco's area–scaled stimuli (likely exhibiting complete spatial summation) were used. On this basis, it was suggested that perimetric stimuli designed to probe altered spatiotemporal summation in glaucoma (i.e., modulating in area, duration, and luminance to identify changes in spatial and temporal summation) would be capable of boosting test sensitivity (disease signal) by approximately 300% over standard perimetric stimuli.

Spatial summation and temporal summation are fundamental physiological phenomena that underpin detection of perimetric stimuli, and repeatable evidence indicates that they are altered in individuals with retinal degeneration.[51,52,54] In turn, it has been shown[52] (or hypothesized[51,52,61]) that stimuli optimized for accurate and precise identification of these biomarkers boost the disease signal/noise ratio. With this in mind, it is imperative that functional biomarkers for other sight-threatening disease such as AMD are investigated for alterations of spatial and temporal summation, and improvements in the design of perimetric stimuli should be made if it is found that these could be of benefit to disease detection and monitoring. Previous research in spatial and temporal summation in AMD is limited. Brown

and Lovie-Kitchin[62] found altered temporal contrast modulation sensitivity in AMD participants compared to that in age-matched controls. In later research, the same group found the critical duration to be longer in patients with AMD compared to healthy controls, but this difference failed to reach statistical significance.[63] On the basis of this research, it was hypothesized that temporal resolution produces sufficient stress on rod and cone photoreceptors to detect a measurable reduction of sensitivity in AMD, whereas the temporal summation of light photons does not.[63] Notably, temporal summation was not measured under conditions of conventional perimetry; instead, red stimuli of 0.25° diameter were used. Zele and colleagues[64] did not find any change in spatial summation between participants with early or intermediate AMD and healthy controls when examined using Gabor patches of different area. In more recent research, perimetric sensitivity to Goldmann IV and V stimuli was significantly higher in individuals with AMD than in healthy controls (~0.5–1 dB on average) within the central 10°, but not with Goldmann I to III (Choi A, et al. *IOVS*. 2018;59:ARVO Abstract 1260). This implies that spatial summation may be altered (i.e., a change in Ricco's area) in AMD compared to controls. Furthermore, improved structure–function relationships in participants with intermediate AMD have been identified, with perimetric stimuli undergoing complete spatial summation compared to those in which the standard GIII stimulus was used. (Choi A, et al. *IOVS*. 2017;58:ARVO Abstract 4705).

Given the structural changes that occur in AMD at the level of the retina[65–67] and visual cortex,[68–70] we hypothesized that spatial, temporal, and spatiotemporal summation are altered as part of the disease to optimize visual sensitivity in corresponding regions of the visual field. In this study, we examined this hypothesis under the adaptation conditions of clinical perimetry using a custom gaze-contingent test to inform the optimum stimulus parameters for the detection and monitoring of AMD.

Methods

Participants

Twenty participants with early or intermediate dry AMD (mean age, 74.6 years; range, 57–90) and 20 healthy age-similar controls (mean age, 67.8 years; range, 55–80) were recruited for this study. Mean logMAR visual acuities (measured monocularly, with refractive correction in place if required, using an Early Treatment Diabetic Retinopathy Study [ETDRS] chart at 4 m, scoring every letter read correctly) were 0.13 and 0.03 for the control and AMD groups, respectively. All participants were tested in the Centre for Optometry and Vision Science at Ulster University, Coleraine, UK.

Healthy participants had visual acuities of 6/9 (20/30) or better in the test eye (range, 6/5 [20/17]–6/9 [20/30]), and optical coherence tomography (OCT) scans (SPECTRALIS; Heidelberg Engineering, Heidelberg, Germany) of the macular area that were within normal limits. Participants with AMD had visual acuities of 6/12 (20/40) or better in the test eye (range, 6/5 [20/17]–6/12 [20/40]). All participants had spherical refractive error within ±6.00 diopter sphere (DS) in all meridians, with astigmatism ≤ 1.25 diopter cylinder (DC), normal intraocular pressure (>5 and ≤21 mmHg), and OCT-measured peripapillary retinal nerve fiber layer (RNFL) thickness within normal limits. Full visual fields were confirmed in the test eye with the 24-2 SITA Standard test on the Humphrey Field Analyzer 3 (Carl Zeiss Meditec, Dublin, CA), in addition to the absence of any systemic disease that may affect visual performance in both healthy control and AMD participants. Slit-lamp assessment of the anterior eye and biomicroscopic assessment of the posterior segment revealed no ocular pathology in control participants or concurrent ocular abnormalities in AMD participants. All participants had clear media as examined using the slit lamp.

Characteristic features of AMD including drusen and hypo- or hyperpigmentary abnormalities were confirmed using SPECTRALIS OCT (en face infrared images and B-scans) and chromatic retinal photography of the macular area in AMD participants (CR-DGi Non-Mydriatic Fundus Camera, viewing angle, 40°; Canon, Tokyo, Japan). The Beckman clinical classification system[71] (Table 1) was used to grade the severity of AMD evident in fundus photographs. Any eyes displaying signs of neovascular AMD were excluded from psychophysical testing.

Ethical approval to undertake this study was granted by the Health and Social Care Research Ethics Committee A. The research protocol adhered to the tenets of the Declaration of Helsinki, and each participant provided informed consent prior to data collection.

Apparatus and Stimuli

Stimuli were circular achromatic increments presented on a gamma-corrected CRT display (420GS; frame rate, 75 Hz; pixel resolution, 1280 × 1024;

Table 1. Beckman AMD Clinical Classification System[71]

Classification of AMD	Definition (Lesions Assessed Within 2 Disk Diameters of Fovea in Either Eye)
No apparent aging changes	No drusen *and* no AMD pigment abnormalities[a]
Normal aging changing	Only drupelets (small drusen, ≤63 µm in diameter) *and* no AMD pigment abnormalities[a]
Early AMD	Medium drusen (>63 µm but ≤125 µm in diameter) *and* no AMD pigment abnormalities[a]
Intermediate AMD	Large drusen (>125 µm in diameter) *and/or* any pigment abnormalities[a]
Late AMD	Neovascular AMD *and/or* any geographic atrophy[a]

[a]AMD pigment abnormalities include any definite hyper- or hypopigmentary abnormalities associated with medium or large drusen but not associated with known disease entities.

viewing distance, 64 cm; maximum luminance, 122.7 cd/m^2; Sony, Tokyo, Japan) with a uniform gray background luminance of 9.62 cd/m^2 following a 1-hour warm-up period. MATLAB R2016b (MathWorks, Natick, MA) with Psychtoolbox 3.0 and Bits+ (Cambridge Research Systems, Rochester, UK) were used to generate the stimuli. Participants fixated an annulus target (white 0.45°-diameter spot with a central zero-contrast 0.23°-diameter spot) throughout each test. Eye movements were recorded with a high-speed eye tracker (EyeLink 1000 Plus, 1000 Hz; SR Research, Ottawa, ON, Canada) while participants placed their head on a secure, purpose-built chin rest. The eye-tracking system was calibrated and subsequently validated for each observer prior to examination, with data collection being undertaken in normal room illumination to minimize pupil size and limit tracking artifacts secondary to changes in the measured position of the pupil center as a result of variations in pupil size.[72,73] Stimulus presentation position was corrected according to participant gaze position within each frame of presentation (i.e., fully gaze contingent). Where fixation errors were greater than 1° from the fixation target location, any stimulus presentation coinciding with the error was skipped (and repeated later in the test) to prevent stimuli from being presented on monitor locations where spatial luminance inhomogeneity was present or, in the case of large fixation errors, off the monitor screen. Although we did not examine if any participant with AMD was using an eccentric PRL, it is unlikely that this was the case in the cohort we examined because all AMD participants had a visual acuity of 6/12 or better.[74] Responses were collected via a response box (RB-540; Cedrus, New York, NY) with a listening window of 2 seconds. Refractive error was corrected for the test eye and for the experimental working distance, if required, with a trial frame holding a full-aperture lens while an opaque patch was used to occlude the fellow eye.

Experiments were undertaken in two phases, either within a single study visit or in two shorter visits within 1 to 2 weeks of each other. In the first phase, participants performed an area-modulation detection task with a stimulus of constant contrast ($\Delta I = 3.63$ cd/m^2 and $\log \Delta I/I = -0.42$, chosen on the basis of the expected contrast at threshold for Ricco's area–scaled stimuli in healthy observers[52]) and duration (Bridgeman[75] duration, 190.4 ms; 15 frames) but varying in area. This task was used to estimate the localized area of complete spatial summation (Ricco's area) at eight test locations along the 90°, 180°, 270°, and 360° meridians—four each at 2.5° and 5° visual field eccentricities (Fig. 1). Test locations were chosen based on previous psychophysical evidence for the greatest reductions in visual function to occur at parafoveal locations in AMD.[76–80]

In the second phase of experiments, spatiotemporal summation was investigated through the measurement of achromatic contrast thresholds for six stimuli of different durations (1–15 frames; Bridgeman duration, 3.7–190.4 ms), with a GIII stimulus and, separately, a stimulus with an area scaled to the local Ricco's area (thresholds from phase one) at the same locations used in phase one (Fig. 1). All stimuli were presented in a randomized order for all participants. Temporal summation functions were subsequently produced for both stimulus areas at each test location. Regular breaks were provided at intervals throughout data collection and when requested by the participant.

Psychophysical Procedure

Thresholds for area (phase one) and contrast (phase two) were measured with a randomly interleaved 1/1 staircase with a yes/no response paradigm. Each staircase terminated after four reversals, with thresholds being calculated as the mean of the final two reversals

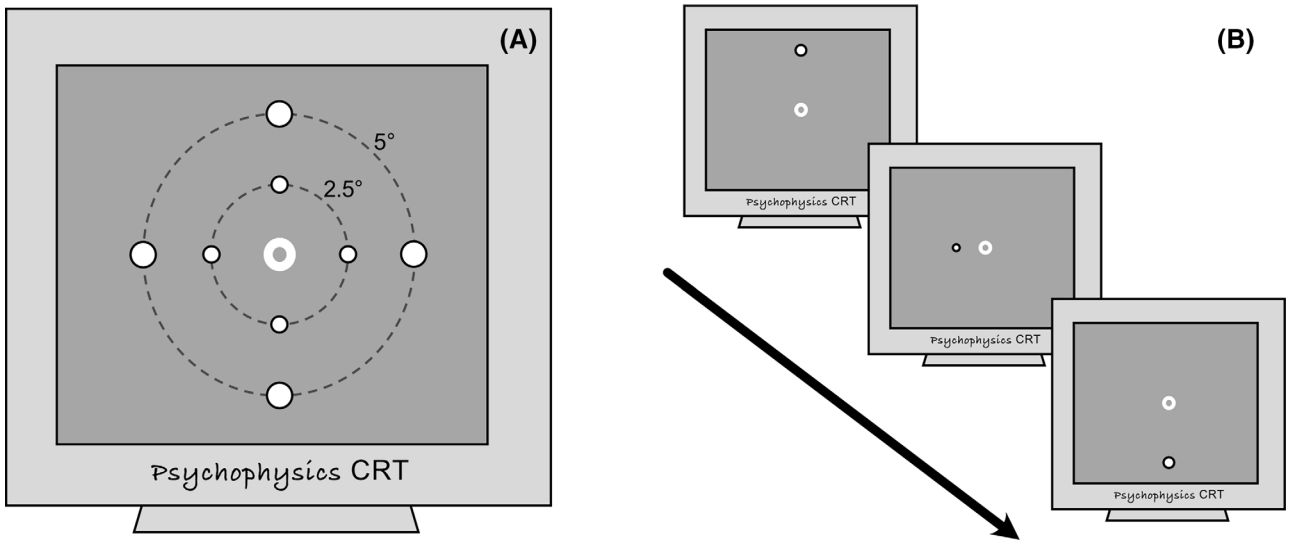

Figure 1. Schematic to demonstrate (**A**) stimuli presented at all test locations examined, and (**B**) test sequence.

for area (phase one) and the mean of all four reversals for contrast (phase two). In phase one, stimulus diameter was varied by 20% when fewer than two reversals had occurred, by 10% when two reversals were reached, and by 5% when two reversals were exceeded. In phase two, contrast was varied by 0.5 log unit steps when reversals were below two, by 0.25 log units when two reversals had occurred, and by steps of 0.05 log units for greater than two reversals. Stimulus area or contrast was modulated according to participant response (i.e., increased when "unseen" and decreased when "seen"). False-positive responses were recorded as those occurring within 100 ms of stimulus onset. If the false-positive rate exceeded 20% for any given test, the data were discarded and the test run was repeated later in the experimental session at a randomly determined point. Prior to beginning each phase of data collection, each participant undertook a trial run and only proceeded with study measurements when the test was clearly understood.

Data Analysis

Area-Modulation Data

Threshold area values (Ricco's area estimates) were compared between healthy control and AMD participants for each individual test location. To test for statistically significant differences, a Wilcoxon rank-sum test was performed, with post hoc Holm–Bonferroni correction used to account for multiple tests of the same hypothesis at different stimulus locations examined for each participant and to control for independence. The relationships between mean measures of logMAR visual acuity and mean area thresholds in each observer were also examined at 2.5° and 5° eccentricities using Spearman's correlation.

Temporal Summation Data

Thresholds were expressed as increment energy values (ΔE, cd/m^2·s·deg^2) and were calculated as the product of increment luminance (cd/m^2), stimulus duration (s), and stimulus area (deg^2). Stimulus durations were converted to Bridgeman equivalents[75] and verified with an optical transient recorder (OTR-3; Display-Metrology & Systems, Karlsruhe, Germany). When a participant was unable to detect a stimulus with the maximum contrast, data from that location were excluded from further analysis. To determine temporal summation functions, log stimulus energy was plotted against log stimulus duration. Iterative two-phase regression analysis[81] (Levenberg–Marquardt estimation with a maximum of 5000 iterations) was then used to estimate the critical duration at individual test locations under all conditions for each observer. Briefly, two lines were fitted to the data, with the slope of the first line constrained to 0 (representing complete temporal summation in line with Bloch's law) but the slope and intercept of the second line (representing partial summation) being free to vary between 0 and 1. The point on the duration axis at which the two lines in the function intersected (breakpoint) was taken as the critical duration estimate for that location. In cases where critical duration estimates were less than the shortest stimulus duration (one frame, 3.7 ms) or where marked variability in the data caused the two-phase regression analysis to fail, these data were excluded from

further analysis. Where critical duration estimates were greater than the longest stimulus duration (15 frames, 190.4 ms), these values were substituted with a value of 190.4 ms (2.28 log ms) for further analysis.

A Wilcoxon rank-sum test with subsequent Holm–Bonferroni correction was used to test for statistically significant differences in the critical duration estimates between healthy controls and AMD participants at each test location when the GIII stimulus and the Ricco's area–scaled stimuli were used. Differences in the slopes of the second line of all temporal summation functions (partial summation) between controls and AMD participants were also tested for with a Wilcoxon rank-sum test and subsequent Holm–Bonferroni correction.

The mean difference in log energy thresholds between each control and AMD observer, otherwise termed the *disease signal*, was calculated for all stimulus durations with the GIII stimulus and Ricco's area–scaled stimuli at 2.5° and 5° visual field eccentricities. A three-way analysis of variance (ANOVA) with the fixed effects of stimulus condition (GIII or Ricco's area–scaled stimuli), stimulus duration, and visual field eccentricity was used to identify factors influencing the disease signal. This analysis was supplemented by the construction of receiver operating characteristic (ROC) curves and calculation of associated area under the ROC curve (AUC) values at 2.5° and 5°. Then, 95% confidence intervals for each ROC curve were generated using 2000 stratified bootstrap replicates. AUC values were used to compare the relative ability of standard perimetric stimuli (GIII stimulus with fixed duration of 190.4 ms, modulating in luminance) and an area-modulation test (using a stimulus of fixed contrast and duration of 190.4 ms) for diagnostic accuracy in the detection of AMD. Permutation analysis was subsequently used to determine if observed differences in AUC values with each stimulus form at each eccentricity were statistically significant. In short, this required threshold data for each stimulus form to be randomly reassigned to two groups (without replacement) that were matched in size to the initial variables. When this had been done, two ROC curves and AUC values were generated for each random group and differences between AUC values calculated. This process was repeated 5000 times to create a distribution of random AUC differences. A two-sided P value was then calculated for the observed differences in AUC values at each eccentricity.

For all statistical tests, an α-value (two-tailed) of 0.05 (after correction for multiple comparisons as appropriate) was considered statistically significant.

Results

In total, nine eyes with early AMD, 10 with intermediate AMD, and one eye with non-central geographic atrophy (diameter, 0.08°), in addition to 20 healthy control eyes, were included in data analysis. Temporal summation measurements with the Ricco's area–scaled stimuli could not be acquired in one participant with intermediate AMD due to poor fixation and concentration. However, all other study measurements were successfully obtained.

Spatial Summation

Localized area-modulation thresholds (Ricco's area estimates) were measured in all 20 participants with AMD and 20 healthy controls. Ricco's areas were significantly larger in AMD participants compared to healthy controls at each individual test location (all $P < 0.05$, Wilcoxon rank-sum test) (Fig. 2). Summary values for spatial summation measurements in observers with AMD compared to healthy controls are shown in Table 2. We also observed statistically significant increases in area thresholds for AMD participants with intermediate compared to early disease at each eccentricity (all $P < 0.05$, Wilcoxon

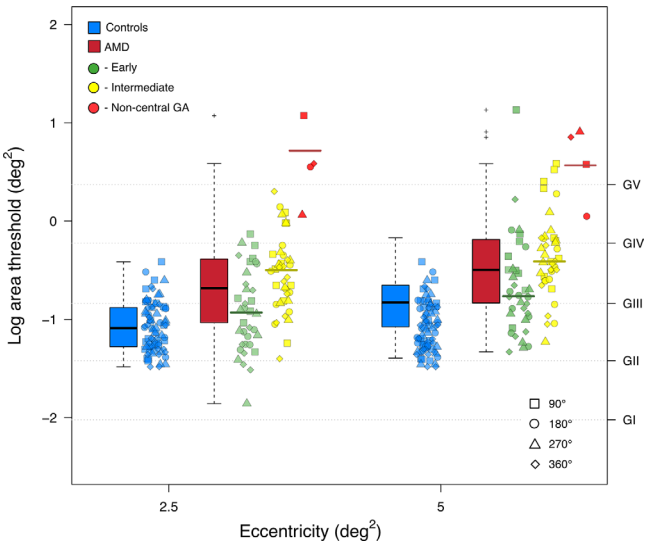

Figure 2. Boxplots of Ricco's area estimates at 2.5° and 5° visual field eccentricities (pooled across all test locations) for healthy controls (*blue*) compared to AMD participants (*red*). The lower and upper limits of the boxes represent the 25th and 75th percentiles of the data, respectively. The *error bars* extend to the most extreme data point within 1.5× the IQR from the top and bottom of the box. Individual data points for individual observers at each test location are included for reference and color-coded according to disease severity (median area thresholds for the severity groups are represented by *horizontal lines*).

Table 2. Ricco's Area and Critical Duration Estimates at Each Visual Field Eccentricity for Healthy Control and AMD Participant Groups

Parameter	Eccentricity (deg)	Participant Group, Median (IQR)		*P*
		Controls	AMD	
Ricco's area (deg^2)	2.5	0.081 (0.05–0.13)	0.208 (0.09–0.41)	**<0.001**
	5.0	0.148 (0.08–0.22)	0.319 (0.15–0.65)	**0.025**
GIII critical duration (ms)	2.5	17.0 (10.1–23.5)	17.9 (9.3–30.4)	0.717
	5.0	17.0 (12.1–25.0)	20.6 (13.2–30.4)	0.858
Ricco's area–scaled critical duration (ms)	2.5	21.1 (11.8–33.9)	25.3 (17.0–42.0)	0.329
	5.0	23.4 (15.6–32.7)	18.2 (11.2–38.2)	0.355

The *P* values are for the statistical comparisons of Ricco's area and critical durations estimates between AMD and healthy control participant groups. Statistically significant *P* values are indicated in bold.

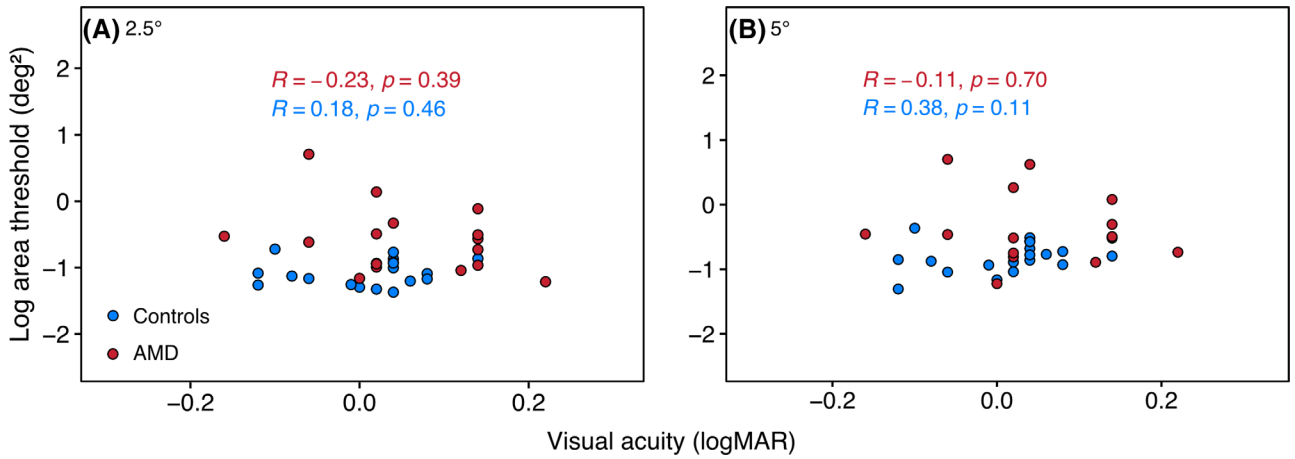

Figure 3. Plots of logMAR visual acuity at fixation against Ricco's area estimates at (**A**) 2.5° and (**B**) 5° visual field eccentricities in controls (*blue*) and AMD participants (*red*).

rank-sum test). Weak relationships that failed to reach statistical significance (all $P > 0.05$) were observed between visual acuity (logMAR) and Ricco's area estimates at both 2.5° and 5° in control observers and participants with AMD (Fig. 3).

Temporal Summation

Log energy thresholds (median, IQR) were higher in AMD participants compared to controls for both the GIII and Ricco's area–scaled stimuli at 2.5° and 5° eccentricities for all stimulus durations and at each test location (all $P < 0.001$, Wilcoxon rank-sum test) (Fig. 4).

In healthy observers, 160 local temporal summation measurements were generated, each with the GIII and Ricco's area–scaled stimuli. In total, 153 temporal summation functions were successfully fitted for the GIII stimuli and 157 for the Ricco's area–scaled stimuli. For AMD participants, 160 local temporal summation measurements were acquired with the GIII stimulus and 152 with the Ricco's area–scaled stimuli. A total of 134 temporal summation curves were successfully fitted to threshold measurements with the GIII stimulus and 135 with the Ricco's area–scaled stimuli in AMD participants.

Although critical duration values were longer in AMD participants compared to those in healthy controls with the GIII stimulus at 2.5° (AMD: 17.9 ms, IQR = 9.3–30.4; controls: 17.0 ms, IQR = 10.1–23.5) and 5° (AMD: 20.6 ms, IQR = 13.2–30.4; controls: 17.0 ms, IQR = 12.1–25.0), these differences were not found to be statistically significant (all $P > 0.05$, Wilcoxon rank-sum test) (Table 2). Similarly, the critical duration was longer in AMD participants at 2.5° with Ricco's area–scaled stimuli (AMD: 25.3 ms, IQR = 17.0–42.0; controls: 21.1 ms, IQR = 11.8–33.9), but this was not statistically significant ($P = 0.329$) (Table 2). Conversely, a non-significant ($P = 0.355$) shortening of the critical

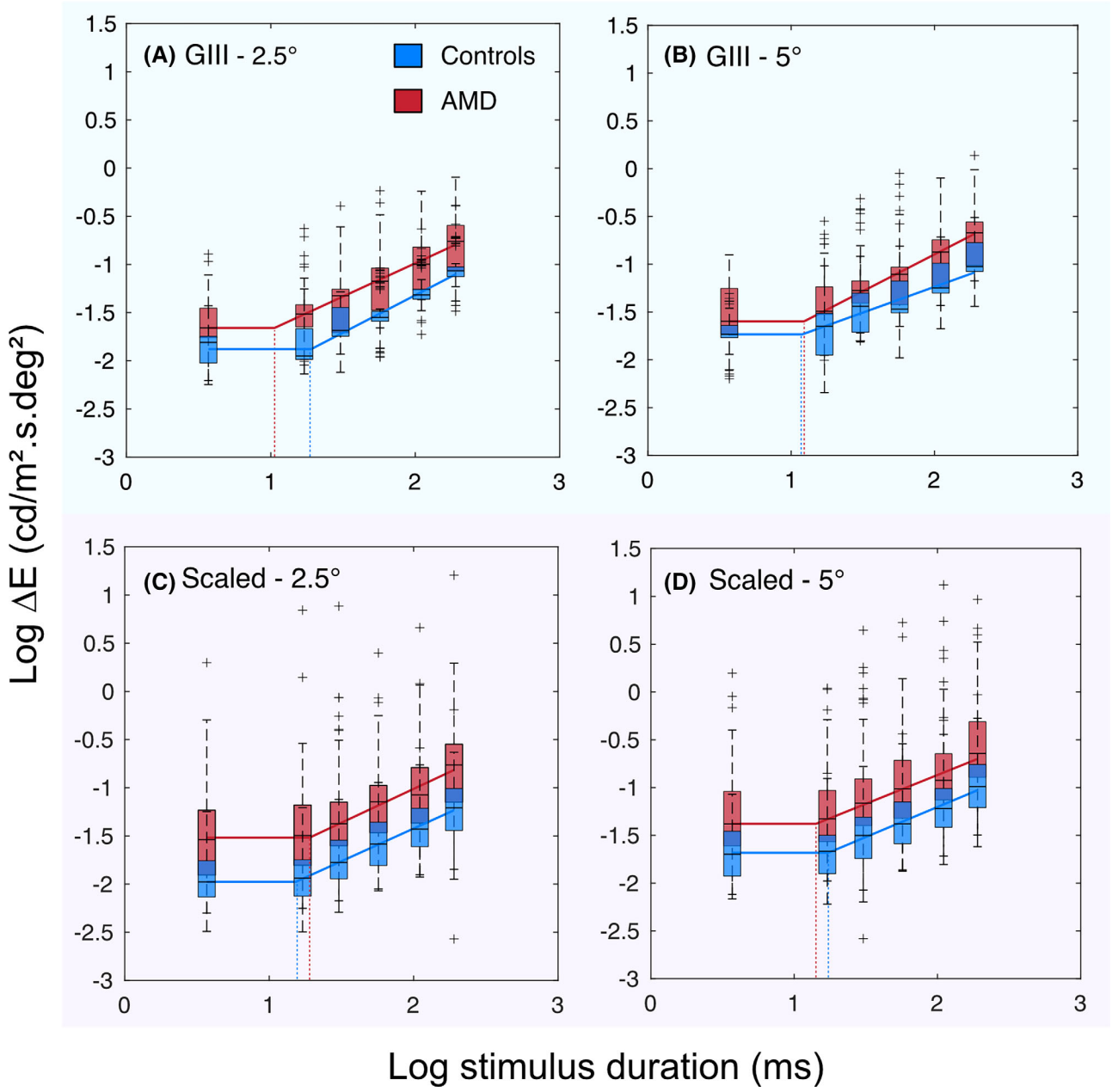

Figure 4. Contrast thresholds measured for six stimulus durations with a GIII stimulus (**A**, **B**; *blue shading*) and stimuli scaled to the localized Ricco's area (**C**, **D**; *purple shading*) in healthy controls (*blue*) and participants with AMD (*red*). Temporal summation functions fitted to median threshold values are also included in each plot. The *dashed line* to the *x*-axis represents the critical duration.

duration was observed at 5° with the Ricco's area–scaled stimuli (AMD: 18.2 ms, IQR = 11.2–38.2; controls: 23.4 ms, IQR = 15.6–32.7). Boxplots reporting critical duration values at 2.5° and 5° visual field eccentricities tested under both stimulus conditions for AMD and healthy control participants are shown in Figure 5.

Finally, partial summation, quantified by the second line slope of temporal summation functions, was not significantly different between AMD and healthy participants with the GIII stimulus (all $P > 0.05$, Wilcoxon rank-sum test) at 2.5° (AMD: 0.80, IQR = 0.70–0.91; controls: 0.79, IQR = 0.66–0.88) and 5° (AMD: 0.79, IQR = 0.66–0.89; controls: 0.81, IQR = 0.64–0.89) eccentricities. Similarly, no statistically significant differences in second-line slope values between controls and AMD observers were found with Ricco's area–scaled stimuli (all $P > 0.05$, Wilcoxon rank-sum test) at 2.5° (AMD: 0.79, IQR = 0.64–0.95; controls: 0.77, IQR = 0.67–0.88) or 5° (AMD: 0.74, IQR = 0.57–0.94; controls: 0.79, IQR = 0.61–0.89) eccentricities.

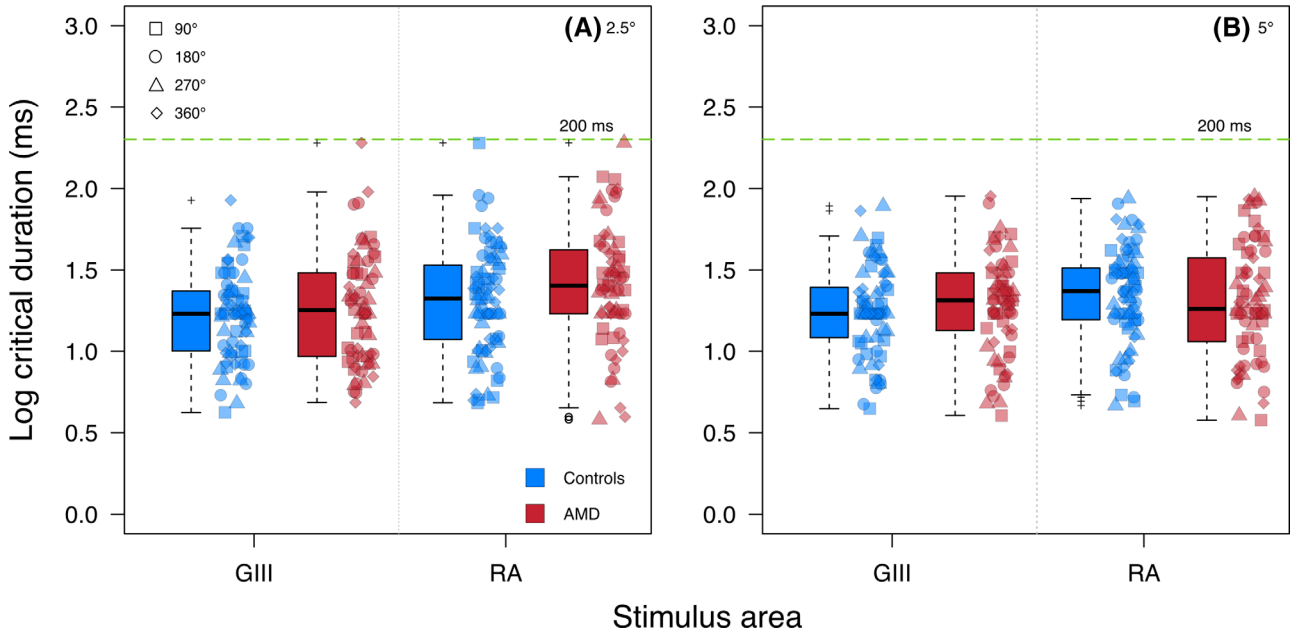

Figure 5. Critical duration estimates at 2.5° (**A**) and 5° (**B**) visual field eccentricities for healthy controls (*blue*) and participants with AMD (*red*) with a GIII stimulus and Ricco's area–scaled stimuli. Outliers are represented by "+" markers.

Disease signal (mean log energy threshold difference between each control and AMD participants) was higher with Ricco's area–scaled stimuli compared to the GIII stimulus for all stimulus durations at both 2.5° and 5° visual field eccentricities (Figs. 6A, 6B). A three-way ANOVA revealed no statistically significant interaction effects among stimulus condition, stimulus duration, and visual field eccentricity on disease signal (all $P > 0.05$). Main effect analysis demonstrated that the disease signal was higher with Ricco's area–scaled stimuli compared to the GIII stimulus ($P < 0.001$). Post hoc analysis showed a statistically significant improvement in disease signal with Ricco's area–scaled stimuli compared to the GIII stimulus for all stimulus durations at each test location (all $P < 0.001$, paired *t*-test). A similar trend was also observed with ROC curves and associated AUC values (Figs. 6C, 6D) whereby a statistically significantly larger ($P < 0.001$) AUC value was found using stimuli capable of probing changes in spatial summation in AMD (area modulation stimulus, 190.4 ms) relative to the standard perimetry stimulus (GIII, 190.4 ms).

Discussion

This study found that estimates of Ricco's area are significantly larger in participants with dry AMD than in healthy controls. To the best of our knowledge, this is the first study to demonstrate changes in the spatial summation characteristics of individuals with dry AMD under the conditions of photopic gaze-contingent perimetry. No changes in temporal summation (critical duration) were observed when either a GIII stimulus or stimuli scaled to the local Ricco's area were used.

Findings from previous research have suggested that Ricco's area may be larger in AMD as a result of significant differences in the hill of vision between AMD patients and controls when measured with Goldmann IV and V stimuli, but no significant differences with Goldmann I, II, and III stimuli (Choi A, et al. *IOVS*. 2018;59:ARVO E-Abstract 1260). Consistent with this hypothesis, we found estimates of Ricco's area to be between those of Goldmann III (0.147 deg^2) and IV (0.59 deg^2) stimuli in AMD participants, and between Goldmann II (0.037 deg^2) and III stimuli in healthy participants at 2.5° and 5° visual field eccentricities (Table 2) for a similar adaptation luminance (9.62 cd/m^2). In contrast with the present study, Zele and colleagues[64] did not find a change in cone-mediated spatial summation in four participants with AMD when tested with a contrast-modulating Gabor stimulus matched to the optimal contrast detector. Marked differences in both the stimuli and method used to plot spatial summation functions (constraining both lines in bilinear fit to reflect partial and no summation) do, however, confound comparisons with the current study. It may be further argued that the use of stimuli probing cone function may not reveal functional deficits related to the loss or damage of rod photoreceptors (reported

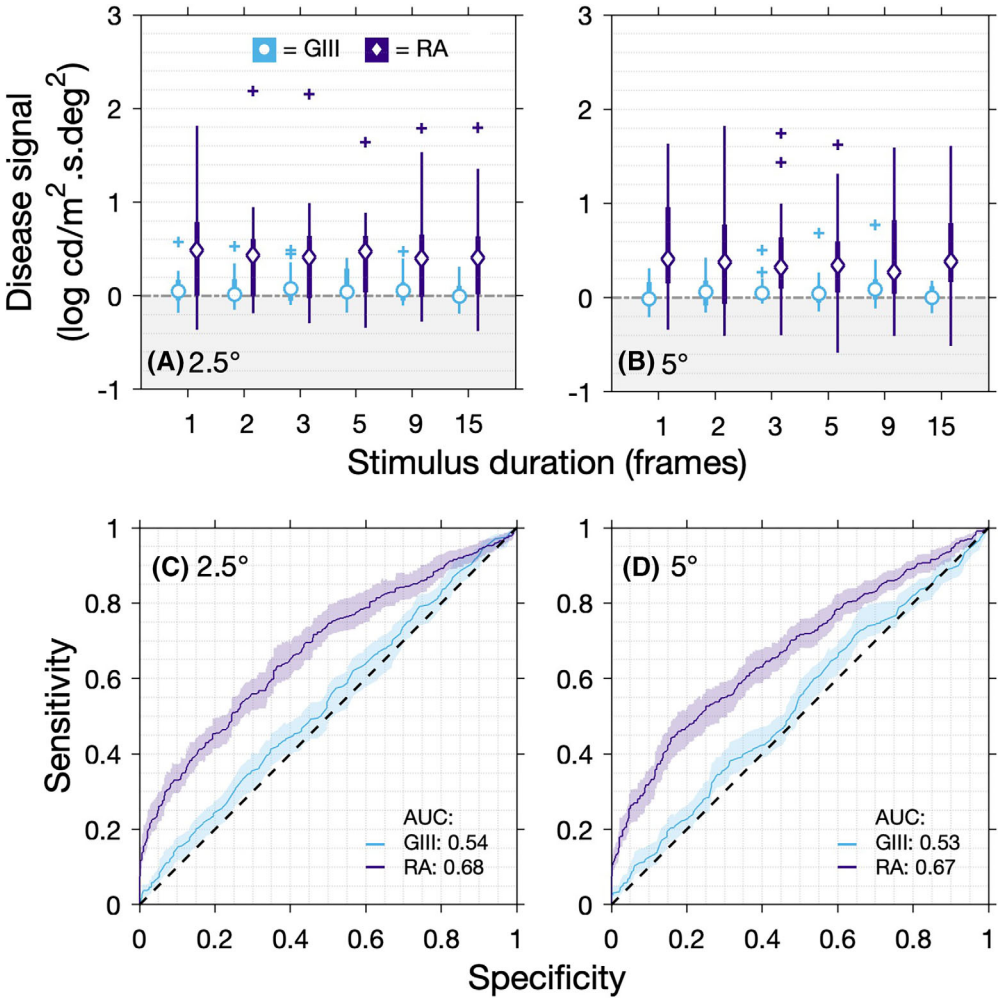

Figure 6. Mean disease signal (mean log energy threshold difference between AMD and control participants) for all six stimulus durations with the GIII stimulus (*blue*) compared to Ricco's area (RA)–scaled stimuli (*purple*) at 2.5° (**A**) and 5° (**B**) visual field eccentricities. Outliers are represented by "+" markers. ROC curves indicating the ability of the GIII stimulus (*blue*) compared to RA-scaled stimuli of 15-frame duration (190.4 ms) to discriminate between AMD and control eyes are presented for 2.5° (**C**) and 5° (**D**) visual field eccentricities. Associated AUC values and 95% confidence intervals (*shaded regions*) are included on each plot (see Methods).

to be predominantly affected early in the AMD disease process[82]).

Changes in spatial summation in AMD may also be inferred from studies examining other forms of spatial vision in the disease. Shah et al.[83] found visual acuity measures with novel pseudo-high-pass–filtered optotypes to be reduced to a greater extent in early AMD compared to measures using conventional high-contrast optotypes. This finding was hypothesized to be related to altered neural sampling secondary to the loss of photoreceptors, with the result that visual acuity measures in the fovea are limited by neural rather than optical factors. Such results may also be hypothesized to be related to an enlargement in Ricco's area, serving to optimize local sensitivity at the expense of spatial resolution. In AMD, where structural changes are likely to be inhomogeneous, this will result in a reduced density sampling array that will affect resolution thresholds for high-pass-filtered optotypes more than conventional unfiltered optotypes. In a similar manner, the finding of an improved structure–function relationship in AMD when microperimetry is undertaken in mesopic and scotopic conditions may also potentially be explained by a change in spatial summation in the disease. Specifically, if both healthy and AMD patients exhibit complete spatial summation with the standard GIII stimulus under mesopic and scotopic conditions, it is likely that such differences in Ricco's area are more measurable because of a greater separation of the spatial summation curves at this point.

Only one previous study has examined temporal summation in AMD. Similar to the current study, Brown and Lovie-Kitchin[63] reported that the critical

duration, measured under photopic conditions with a red 0.25°-diameter spot stimulus, was longer in AMD observers compared to that in controls, but their finding was not statistically significant. In terms of critical duration estimates, Brown and Lovie-Kitchin[63] found these to be substantially longer for both the controls (58 ms) and the AMD (92 ms) groups compared to the same groups in this study. Such differences are likely related to variations in the stimulus area used and stimulus chromaticity, in addition to our use of photopic conditions to optimize the accuracy of the gaze-contingent system used.[58] It is also worth noting that Brown and Lovie-Kitchin[63] used a method of analysis to estimate the critical duration that fits two lines of constrained slope to the data reflecting complete and no summation; this method is known to give longer critical duration estimates compared to those measured using iterative two-phase regression analysis[84] used in the present study.

Physiological Source of Altered Spatial Summation in AMD

Although the physiological basis for Ricco's area is uncertain, it has been hypothesized that RGC receptive field organization,[85,86] photoreceptor and RGC density,[48,87] and cortical receptive field characteristics[45,53,88] contribute to determining the size of Ricco's area. It would thus follow that, if the functioning of these anatomical loci is affected by a given disease process or non-pathological change (e.g., alterations in adapting luminance), then Ricco's area would also be altered in size to optimize visual sensitivity in a given region of the visual field. In the case of dry AMD, it is possible that disruption to the photoreceptor mosaic due to the accumulation of lipid-rich extracellular material (drusen) between the aging retinal pigment epithelium (RPE) and Bruch's membrane,[89–91] degeneration and dysfunction of rod and later cone photoreceptors,[92] RPE loss,[93] reticular pseudodrusen,[94] alterations in receptive field organization,[85,86] and cortical changes[70,95,96] potentially contribute to altered spatial summation in the disease. This disruption may also increase as dry AMD progresses, because Ricco's area has been found to scale with disease severity (Fig. 6).

A number of studies have demonstrated that dark-adapted microperimetry is more effective at detecting functional deficits in early AMD. It has been hypothesized that this is related to the capability of such tests to probe photoreceptor loss early in the disease process. Ricco's area is larger under scotopic than photopic conditions, and it is therefore likely that thresholds for a GIII stimulus are determined by complete spatial summation across a larger area of the visual field. Operating under complete spatial summation may, in part, account for the improved sensitivity of dark-adapted microperimetry to the effects of AMD. Despite this, it is unlikely that altered photoreceptor function or density solely accounts for changes in spatial summation in the disease. Although it is acknowledged that stimuli designed to isolate and probe spatial summation in individual classes of photoreceptors (e.g., S- and L-cone) do yield different Ricco's area measures in healthy observers, the non-uniform relationship between the density of individual photoreceptors and alterations in corresponding Ricco's area measures within the central 20° suggests that receptive fields beyond those of the photoreceptors likely determine the extent of Ricco's area.[47] Research by Tuten et al.[97] found that Ricco's area was unchanged when measured with and without adaptive optics to minimize the effects of higher order aberrations and retinal image motion. Were this to be primarily related to photoreceptor density, Ricco's area would be expected to be smaller when retinal image motion was accounted for. Considering such evidence, it is likely that changes in the structure and/or function of post-receptoral pathways in response to retinal changes explain our observation of altered estimates of Ricco's area in AMD.

In healthy eyes, the number of RGCs underlying Ricco's area has been demonstrated to be relatively constant (~14–32 RGCs),[48,87] with the result that variations in Ricco's area with visual field eccentricity in photopic conditions may mostly be accounted for by alterations in RGC density. Glaucoma-induced changes in Ricco's area have also been hypothesized to develop to maintain input to cortical receptive fields from a constant number of RGCs, thus maintaining a constant signal-to-noise ratio. Although it is known that RGCs contribute to determining the size of Ricco's area, some debate surrounds the effect of AMD on RGC density. In a clinicopathologic assessment of eyes with dry and neovascular AMD, Medeiros and Curcio[98] reported marked rod photoreceptor loss, but RGC density appeared to be preserved in dry AMD, only becoming affected in the end-stage neovascular forms of the disease. Later research demonstrated that inner retinal thickness (e.g., inner plexiform layer, ganglion cell complex, peripapillary RNFL thickness) is significantly thinner in patients with dry AMD.[99–102] If the functional RGC number were to be reduced in AMD, it is possible that spatial summation also changes in an attempt by the visual system to optimize visual function in response to insult.

Alterations in retinal structure may also be accompanied by change in higher visual centers in AMD,

which could also partly explain our findings. A number of studies have identified evidence for large-scale reorganization of the visual cortex in individuals with macular degeneration such that peripheral stimuli activate the foveal cortex. The extent of any reorganization would be dependent on the extent of vision loss and disease chronicity.[70,95,96] Changes in the size of cortical receptive fields in response to retinal damage have also been demonstrated in both animal models of disease and other retinal degenerations in human observers. For example, Gilbert and Wiesel[103] applied laser burns to the retina that caused an increase in the diameter of cortical receptive fields near the edge of the scotoma to be subsequently detected. Later research by Baseler et al.[104] reported that population receptive fields (pRFs) were significantly larger in regions of the visual cortex corresponding to retinal damage in patients with AMD or Stargardt disease when compared with control observers. Interestingly, similar changes in pRF size were observed in healthy observers when measures were undertaken with stimuli masked to simulate AMD damage.

Given the intrinsic linkages between spatial and temporal summation,[105] it is curious that no concurrent change in the critical duration was observed when a GIII stimulus and Ricco's area–scaled stimuli were used. Previous research has resulted in the hypothesis that altered temporal summation in conditions such as glaucoma may be related to RGC-specific dysfunction and/or alterations in the temporal properties of receptive fields in higher visual centers (e.g., visual cortex). If indeed these processes do underpin altered temporal summation in other diseases, such processes do not appear to be at play in AMD. Brown and Lovie-Kitchin[62,63] found no changes in the critical duration but did report altered temporal discrimination in AMD; they proposed that the processes responsible for temporal summation may be more resistant to degenerative damage caused by AMD compared to those moderating temporal discrimination. In a similar manner, the processes or anatomical locations determining the size of Ricco's area in AMD may be preferentially damaged in early/intermediate disease while sparing those responsible for temporal summation.

Implications for Perimetric Assessment of AMD

The relatively larger Ricco's areas in dry AMD compared to those in healthy controls, as presented in this work, indicate that the standard photopic perimetry test with a GIII stimulus modulating in luminance may not be optimal for the detection and monitoring of visual function in early–intermediate AMD. The effect of using a stimulus scaled to the local Ricco's area, rather than a conventional GIII stimulus, may be seen in the plot of disease signal in Figure 6 (expressed as the mean difference in log energy thresholds between each control and AMD observer). It is clear that the disease signal (i.e., test sensitivity) was consistently higher for the Ricco's area–scaled stimuli at both 2.5° and 5° and remained relatively constant with changes in stimulus duration. Using ROC curves, we also observed that stimuli capable of probing changes in spatial summation in AMD exhibit larger AUC values for AMD detection compared to conventional stimuli. It may, however, also be noted that, although larger, AUC values for the novel area-modulation test (stimulus duration 190.4 ms) were smaller than those required for a diagnostic test (typically > 0.80). This may be accounted for by the fact that disease-related changes were not observed at all locations in the AMD cohort, so "normal" locations are also within this dataset. It should also be noted that AUC values will likely change with disease stage. It is anticipated that, in early AMD where Ricco's area is smaller than the standard GIII stimulus, stimuli capable of probing summation changes will have larger AUCs compared to conventional stimuli. This value would become equal in moderate–late disease where Ricco's area is equal to or exceeds the GIII stimulus area. Furthermore, it should be highlighted that these AUC measures do not represent a final test (e.g., with associated optimized thresholding algorithm) and as such are used very much in an exploratory manner.

Although the outcomes of this work indicate that a stimulus designed to probe changes in spatial summation would optimize perimetric test sensitivity to the effects of dry AMD, further work is necessary to determine if this is also observed in wet AMD and if the boost in test sensitivity is offset by a related increase in test measurement variability (noise). It is also necessary to identify if using perimetric strategies to probe alterations in spatial summation in AMD do indeed offer a more favorable ratio of disease signal to measurement noise in all stages of disease. Furthermore, although all AMD patients in this study had a visual acuity where PRL adoption would not be anticipated,[74] future work is required to completely exclude this as a factor influencing the findings of this study.

Conclusions

Spatial summation appears to be altered in dry AMD, possibly as a form of noise-compensatory

mechanism to account for retinal damage and secondary disturbances to visual processing in the visual cortex in the disease. No significant difference in temporal summation was found between participants with AMD and healthy controls. The sensitivity of perimetric strategies to detect and monitor functional changes in AMD may be markedly improved if stimuli capable of mapping alterations in spatial summation are used.[56]

Acknowledgments

The authors thank Matt J. Dunn, PhD, and Jonathan T. Erichsen, PhD, for the technical advice they provided in setting up this study.

Supported by a PhD studentship from the Macular Society, United Kingdom (AMLH) and by the National Institute for Health Research Biomedical Research Centre based at Moorfields Eye Hospital NHS Foundation Trust and UCL Institute of Ophthalmology (RSA, DFG-H, PJM). DFG-H's chair at University College London is supported by funding from Glaucoma UK. The views expressed are those of the authors and not necessarily those of the National Health Service, the National Institute for Health Research, or the Department of Health. Conference presentation of this work at the 24th International Visual Field & Imaging Symposium (August 2022; Berkeley, CA) was supported by the Imaging and Perimetry Society in the form of a travel grant (AMLH).

Disclosure: **A.M.L. Hunter,** None; **R.S. Anderson,** visual field sensitivity testing (P), Alliance Pharmaceuticals (R); **T. Redmond,** visual field sensitivity testing (P); **D.F. Garway-Heath,** visual field sensitivity testing (P), Alcon Research Institute (F), Janssen (F, C), Santen UK (F, C), Novartis (F), CenterVue (R, C), Heidelberg Engineering (R), Oculus (R), Topcon (R), Allergan (C), Bausch & Lomb (C), Genentech (C), Omicron (C), Roche (C); **P.J. Mulholland,** visual field sensitivity testing (P), Heidelberg Engineering (F), LKC Technologies (F)

References

1. Flaxman SR, Bourne RRA, Resnikoff S, et al. Global causes of blindness and distance vision impairment 1990-2020: a systematic review and meta-analysis. *Lancet Glob Health*. 2017;5(12):e1221–e1234.
2. Pezzullo L, Streatfeild J, Simkiss P, Shickle D. The economic impact of sight loss and blindness in the UK adult population. *BMC Health Serv Res*. 2018;18(1):1–13.
3. NICE. *Age-Related Macular Degeneration. NICE Guideline [NG82]*. Manchester, UK: National Institute for Health and Care Excellence; 2018.
4. Cheung CMG, Wong TY. Treatment of age-related macular degeneration. *Lancet*. 2013;382(9900):1230–1232.
5. Tah V, Orlans HO, Hyer J, et al. Anti-VEGF therapy and the retina: an update. *J Ophthalmol*. 2015;2015:627674.
6. Kassoff A, Kassoff J, Buehler J, et al. A randomized, placebo-controlled, clinical trial of high-dose supplementation with vitamins C and E, beta carotene, and zinc for age-related macular degeneration and vision loss: AREDS Report No. 8. *Arch Ophthalmol*. 2001;119(10):1417–1436.
7. Chew EY, Clemons TE, SanGiovanni JP, et al. Secondary analyses of the effects of lutein/zeaxanthin on age-related macular degeneration progression: AREDS2 Report No. 3. *JAMA Ophthalmol*. 2014;132(2):142–149.
8. Merry GF, Munk MR, Dotson RS, Walker MG, Devenyi RG. Photobiomodulation reduces drusen volume and improves visual acuity and contrast sensitivity in dry age-related macular degeneration. *Acta Ophthalmol*. 2017;95(4):e270–e277.
9. Constable IJ, Blumenkranz MS, Schwartz SD, Barone S, Lai CM, Rakoczy EP. Gene therapy for age-related macular degeneration. *Asia Pac J Ophthalmol (Phila)*. 2016;5(4):300–303.
10. Rodrigues IA, Sprinkhuizen SM, Barthelmes D, et al. Defining a minimum set of standardized patient-centered outcome measures for macular degeneration. *Am J Ophthalmol*. 2016;168:1–12.
11. Chakravarthy U, Harding SP, Rogers CA, et al. A randomised controlled trial to assess the clinical effectiveness and cost-effectiveness of alternative treatments to inhibit VEGF in age-related choroidal neovascularisation (IVAN). *Health Technol Assess*. 2015;19(78):1–298.
12. Brown DM, Kaiser PK, Michels M, et al. Ranibizumab versus verteporfin for neovascular age-related macular degeneration. *N Engl J Med*. 2006;355(14):1432–1444.
13. Ivandic BT, Ivandic T. Low-level laser therapy improves vision in patients with age-related macular degeneration. *Photomed Laser Surg*. 2008;26(3):241–245.
14. Hogg R, Curry E, Muldrew A, et al. Identification of lesion components that influence visual

function in age related macular degeneration. *Br J Ophthalmol*. 2003;87(5):609–614.
15. Pondorfer SG, Terheyden JH, Heinemann M, Wintergerst MWM, Holz FG, Finger RP. Association of vision-related quality of life with visual function in age-related macular degeneration. *Sci Rep*. 2019;9(1):15326.
16. Seland JH, Vingerling JR, Augood CA, et al. Visual impairment and quality of life in the older European population, the EUREYE study. *Acta Ophthalmol*. 2011;89(7):608–613.
17. Maguire M. Baseline characteristics, the 25-Item National Eye Institute Visual Functioning Questionnaire, and their associations in the Complications of Age-Related Macular Degeneration Prevention Trial (CAPT). *Ophthalmology*. 2004;111(7):1307–1316.
18. Inatomi A. A simple fundus perimetry with fundus camera. *Doc Ophthalmol Proc Ser*. 1979;19:359–362.
19. Nishida Y, Murata T, Yoshida K, Sawada T, Kani K. An automated measuring system for fundus perimetry. *Jpn J Ophthalmol*. 2002;46(6):627–633.
20. Kani K, Ogita Y. Fundus controlled perimetry. *Doc Ophthalmol Proc Ser*. 1979;19:341–350.
21. Crossland MD, Jackson ML, Seiple WH. Microperimetry: a review of fundus related perimetry. *Optometry Rep*. 2012;2(1):e2.
22. Midena E, Radin PP, Convento E, Cavarzeran F. Macular automatic fundus perimetry threshold versus standard perimetry threshold. *Eur J Ophthalmol*. 2007;17(1):63–68.
23. Landa G, Su E, Garcia PMT, Seiple WH, Rosen RB. Inner segment-outer segment junctional layer integrity and corresponding retinal sensitivity in dry and wet forms of age-related macular degeneration. *Retina*. 2011;31(2):364–370.
24. Liu H, Bittencourt MG, Wang J, et al. Retinal sensitivity is a valuable complementary measurement to visual acuity—a microperimetry study in patients with maculopathies. *Graefes Arch Clin Exp Ophthalmol*. 2015;253(12):2137–2142.
25. Vujosevic S, Pucci P, Casciano M, et al. Long-term longitudinal modifications in mesopic microperimetry in early and intermediate age-related macular degeneration. *Graefes Arch Clin Exp Ophthalmol*. 2017;255(2):301–309.
26. Wu Z, Ayton LN, Luu CD, Guymer RH. Relationship between retinal microstructures on optical coherence tomography and microperimetry in age-related macular degeneration. *Ophthalmology*. 2014;121(7):1445–1452.
27. Midena E, Vujosevic S, Convento E, Manfre' A, Cavarzeran F, Pitotto E. Microperimetry and fundus autofluorescence in patients with early age-related macular degeneration. *Br J Ophthalmol*. 2007;91(11):1499–1503.
28. Pfau M, Lindner M, Müller PL, et al. Effective dynamic range and retest reliability of dark-adapted two-color fundus-controlled perimetry in patients with macular diseases. *Invest Ophthalmol Vis Sci*. 2017;58(6):BIO158–BIO167.
29. Steinberg JS, Saßmannshausen M, Fleckenstein M, et al. Correlation of partial outer retinal thickness with scotopic and mesopic fundus-controlled perimetry in patients with reticular drusen. *Am J Ophthalmol*. 2016;168:52–61.
30. Nebbioso M, Barbato A, Pescosolido N. Scotopic microperimetry in the early diagnosis of age-related macular degeneration: preliminary study. *Biomed Res Int*. 2014;2014:671529.
31. Finger RP, Schmitz-Valckenberg S, Schmid M, et al. MACUSTAR: Development and clinical validation of functional, structural, and patient-reported endpoints in intermediate age-related macular degeneration. *Ophthalmologica*. 2019;241(2):61–72.
32. Squirrell DM, Mawer NP, Mody CH, Brand CS. Visual outcome after intravitreal ranibizumab for wet age-related macular degeneration: a comparison between best-corrected visual acuity and microperimetry. *Retina*. 2010;30(3):436–442.
33. Meleth AD, Mettu P, Agrón E, et al. Changes in retinal sensitivity in geographic atrophy progression as measured by microperimetry. *Invest Ophthalmol Vis Sci*. 2011;52(2):1119–1126.
34. Chen FK, Uppal GS, Maclaren RE, et al. Long-term visual and microperimetry outcomes following autologous retinal pigment epithelium choroid graft for neovascular age-related macular degeneration. *Clin Exp Ophthalmol*. 2009;37(3):275–285.
35. Wu Z, Ayton LN, Luu CD, Guymer RH. Microperimetry of nascent geographic atrophy in age-related macular degeneration. *Invest Ophthalmol Vis Sci*. 2015;56(1):115–121.
36. Acton JH, Gibson JM, Cubbidge RP. Quantification of visual field loss in age-related macular degeneration. *PLoS One*. 2012;7(6):e39944.
37. Chen FK, Patel PJ, Xing W, et al. Test–retest variability of microperimetry using the Nidek MP1 in patients with macular disease. *Invest Ophthalmol Vis Sci*. 2009;50(7):3464–3472.
38. Steinberg JS, Saßmannshausen M, Pfau M, et al. Evaluation of two systems for fundus-controlled scotopic and mesopic perimetry in eye with age-

related macular degeneration. *Transl Vis Sci Technol*. 2017;6(4):7.
39. Maynard ML, Zele AJ, Feigl B. Mesopic Pelli–Robson contrast sensitivity and MP-1 microperimetry in healthy ageing and age-related macular degeneration. *Acta Ophthalmol*. 2016;94(8):e772–e778.
40. Liu H, Bittencourt MG, Wang J, et al. Assessment of central retinal sensitivity employing two types of microperimetry devices. *Transl Vis Sci Technol*. 2014;3(5):3.
41. Rohrschneider K, Springer C, Bültmann S, Völcker HE. Microperimetry—comparison between the micro perimeter 1 and scanning laser ophthalmoscope—fundus perimetry. *Am J Ophthalmol*. 2005;139(1):125–134.
42. Nittala MG, Velaga SB, Hariri A, et al. Retinal sensitivity using microperimetry in age-related macular degeneration in an Amish population. *Ophthalmic Surg Lasers Imaging Retina*. 2019;50(9):E236–E241.
43. Concilium Ophthalmologicum Universale. *Perimetric Standards and Perimetric Glossary of the International Council of Ophthalmology*. 1st ed. Dordrecht: Springer; 1979.
44. Ricco A. Relazione fra il minimo angolo visuale e l'intensità luminosa. *Memorie R Accad Sci Lett Modena*. 1877;17:47–160.
45. Redmond T, Zlatkova MB, Vassilev A, Garway-Heath DF, Anderson RS. Changes in Ricco's area with background luminance in the S-cone pathway. *Optom Vis Sci*. 2013;90(1):66–74.
46. Barlow HB. Temporal and spatial summation in human vision at different background intensities. *J Physiol*. 1958;141(2):337–350.
47. Volbrecht VJ, Shrago EE, Schefrin BE, Werner JS. Spatial summation in human cone mechanisms from 0 degrees to 20 degrees in the superior retina. *J Opt Soc Am A Opt Image Sci Vis*. 2000;17(3):641–650.
48. Kwon MY, Liu R. Linkage between retinal ganglion cell density and the nonuniform spatial integration across the visual field. *Proc Natl Acad Sci U S A*. 2019;116(9):3827–3836.
49. Khuu SK, Kalloniatis M. Spatial summation across the central visual field: implications for visual field testing. *J Vis*. 2015;15(1):1–15.
50. Wilson ME. Invariant features of spatial summation with changing locus in the visual field. *J Physiol*. 1970;207(3):611–622.
51. Mulholland PJ, Redmond T, Garway-Heath DF, Zlatkova MB, Anderson RS. Spatiotemporal summation of perimetric stimuli in early glaucoma. *Invest Ophthalmol Vis Sci*. 2015;56(11):6473–6482.
52. Redmond T, Garway-Heath DF, Zlatkova MB, Anderson RS. Sensitivity loss in early glaucoma can be mapped to an enlargement of the area of complete spatial summation. *Invest Ophthalmol Vis Sci*. 2010;51(12):6540–6548.
53. Je S, Ennis FA, Woodhouse JM, Sengpiel F, Redmond T. Spatial summation across the visual field in strabismic and anisometropic amblyopia. *Sci Rep*. 2018;8(1):3858.
54. Swanson WH, Felius J, Birch DG. Effect of stimulus size on static visual fields in patients with retinitis pigmentosa. *Ophthalmology*. 2000;107(10):1950–1954.
55. Stapley V, Anderson RS, Saunders KJ, Mulholland PJ. Altered spatial summation optimizes visual function in axial myopia. *Sci Rep*. 2020;10(1):12179.
56. Rountree L, Mulholland PJ, Anderson RS, Garway-Heath DF, Morgan JE, Redmond T. Optimising the glaucoma signal/noise ratio by mapping changes in spatial summation with area-modulated perimetric stimuli. *Sci Rep*. 2018;8(1):2172.
57. Bloch AM. Experiences sur la vision. *C R Seances Soc Biol Fil*. 1885;37:493–495.
58. Graham CH, Kemp EH. Brightness discrimination as a function of the increment in intensity. *J Gen Physiol*. 1938;21(5):635–650.
59. Saunders RM. The critical duration of temporal summation in the human central fovea. *Vision Res*. 1975;15(6):699–703.
60. Graham CH, Margaria R. Area and the intensity-time relation in the peripheral retina. *Amer J Physiol*. 1935;113(2):299–305.
61. Anderson RS. The psychophysics of glaucoma: improving the structure/function relationship. *Prog Retin Eye Res*. 2006;25(1):79–97.
62. Brown B, Lovie-Kitchin J. Temporal function in age related maculopathy. *Clin Exp Optom*. 1987;70(4):112–116.
63. Brown B, Lovie-Kitchin JE. Temporal summation in age-related maculopathy. *Optom Vis Sci*. 1989;66(7):426–429.
64. Zele AJ, O'Loughlin RK, Guymer RH, Vingrys AJ. Disclosing disease mechanisms with a spatio-temporal summation paradigm. *Graefes Arch Clin Exp Ophthalmol*. 2006;244(4):425–432.
65. Pfau M, Lindner M, Gliem M, et al. Mesopic and dark-adapted two-color fundus-controlled perimetry in patients with cuticular, reticular, and soft drusen. *Eye (Lond)*. 2018;32(12):1819–1830.

66. Tepelus TC, Hariri AH, Al-Sheikh M, Sadda SR. Correlation between mesopic retinal sensitivity and optical coherence tomographic metrics of the outer retina in patients with non-atrophic dry age-related macular degeneration. *Ophthalmic Surg Lasers Imaging Retina*. 2017;48(4):312–318.
67. Roh M, Laíns I, Shin HJ, et al. Microperimetry in age-related macular degeneration: association with macular morphology assessed by optical coherence tomography. *Br J Ophthalmol*. 2019;103(12):1769–1776.
68. Liu T, Cheung SH, Schuchard RA, et al. Incomplete cortical reorganization in macular degeneration. *Invest Ophthalmol Vis Sci*. 2010;51(12):6826.
69. Maniglia M, Soler V, Cottereau B, Trotter Y. Spontaneous and training-induced cortical plasticity in MD patients: hints from lateral masking. *Sci Rep*. 2018;8(1):90.
70. Baker CI, Peli E, Knouf N, Kanwisher NG. Reorganization of visual processing in macular degeneration. *J Neurosci*. 2005;25(3):614–618.
71. Ferris FL, Wilkinson CP, Bird A, et al. Clinical classification of age-related macular degeneration. *Ophthalmology*. 2013;120(4):844–851.
72. Wyatt HJ. The human pupil and the use of video-based eyetrackers. *Vision Res*. 2010;50(19):1982–1988.
73. Wyatt HJ. The form of the human pupil. *Vision Res*. 1995;35(14):2021–2036.
74. Greenstein VC, Santos RAV, Tsang SH, Smith RT, Barile GR, Seiple W. Preferred retinal locus in macular disease: characteristics and clinical implications. *Retina*. 2007;28(9):1234–1240.
75. Bridgeman B. Durations of stimuli displayed on video display terminals: $(n - 1)/f$ + persistence. *Psychol Sci*. 1998;9(3):232–233.
76. Owsley C, Jackson GR, Cideciyan AV, et al. Psychophysical evidence for rod vulnerability in age-related macular degeneration. *Invest Ophthalmol Vis Sci*. 2000;41(1):267–273.
77. Chen C, Wu L, Wu D, et al. The local cone and rod system function in early age-related macular degeneration. *Doc Ophthalmol*. 2004;109(1):1–8.
78. Acton JH, Theodore Smith R, Hood DC, Greenstein VC. Relationship between retinal layer thickness and the visual field in early age-related macular degeneration. *Invest Ophthalmol Vis Sci*. 2012;53(12):7618.
79. Saßmannshausen M, Steinberg JS, Fimmers R, et al. Structure-function analysis in patients with intermediate age-related macular degeneration. *Invest Ophthalmol Vis Sci*. 2018;59(3):1599–1608.
80. Fraser RG, Tan R, Ayton LN, Caruso E, Guymer RH, Luu CD. Assessment of retinotopic rod photoreceptor function using a dark-adapted chromatic perimeter in intermediate age-related macular degeneration. *Invest Ophthalmol Vis Sci*. 2016;57(13):5436–5442.
81. Seber GAF, Wild CJ. *Nonlinear Regression*. New York: John Wiley & Sons; 1989.
82. Curcio C, Medeiros N, Milican C. Photoreceptor loss in age-related macular degeneration. *Invest Ophthalmol Vis Sci*. 1996;37(7):1236–1249.
83. Shah N, Dakin SC, Dobinson S, Tufail A, Egan CA, Anderson RS. Visual acuity loss in patients with age-related macular degeneration measured using a novel high-pass letter chart. *Br J Ophthalmol*. 2016;100(10):1346–1352.
84. Mulholland PJ, Redmond T, Garway-Heath DF, Anderson RS, Anderson RS. Estimating the critical duration for temporal summation of standard achromatic perimetric stimuli. *Invest Ophthalmol Vis Sci*. 2015;56(1):431–437.
85. Glezer VD. The receptive fields of the retina. *Vision Res*. 1965;5(9):497–525.
86. Barlow HB. Summation and inhibition in the frog's retina. *J Physiol*. 1953;119(1):69–88.
87. Swanson WH, Felius J, Pan F. Perimetric defects and ganglion cell damage: interpreting linear relations using a two-stage neural model. *Invest Ophthalmol Vis Sci*. 2004;45(2):466–472.
88. Pan F, Swanson WH. A cortical pooling model of spatial summation for perimetric stimuli. *J Vis*. 2006;6(11):1159.
89. Gass J. Drusen and disciform macular detachment and degeneration. *Trans Am Ophthalmol Soc*. 1972;70:436.
90. Hageman GS, Luthert PJ, Victor Chong NH, Johnson L V., Anderson DH, Mullins RF. An integrated hypothesis that considers drusen as biomarkers of immune-mediated processes at the RPE–Bruch's membrane interface in aging and age-related macular degeneration. *Prog Retin Eye Res*. 2001;20(6):705–732.
91. Crabb JW. The proteomics of drusen. *Cold Spring Harb Perspect Med*. 2014;4(7):a017194.
92. Johnson PT, Brown MN, Pulliam BC, Anderson DH, Johnson LV. Synaptic pathology, altered gene expression, and degeneration in photoreceptors impacted by drusen. *Invest Ophthalmol Vis Sci*. 2005;46(12):4788–4795.
93. Ambati J, Fowler BJ. Mechanisms of age-related macular degeneration. *Neuron*. 2012;75(1):26–39.
94. Ooto S, Ellabban AA, Ueda-Arakawa N, et al. Reduction of retinal sensitivity in eyes with reticular pseudodrusen. *Am J Ophthalmol*. 2013;156(6):1184–1191.

95. Baker CI, Dilks DD, Peli E, Kanwisher N. Reorganization of visual processing in macular degeneration: replication and clues about the role of foveal loss. *Vision Res*. 2008;48(18):1910–1919.
96. Dilks DD, Julian JB, Peli E, Kanwisher N. Reorganization of visual processing in age-related macular degeneration depends on foveal loss. *Optom Vis Sci*. 2014;91(8):e199–e206.
97. Tuten WS, Cooper RF, Tiruveedhula P, et al. Spatial summation in the human fovea: do normal optical aberrations and fixational eye movements have an effect? *J Vis*. 2018;18(8):1–18.
98. Medeiros NE, Curcio CA. Preservation of ganglion cell layer neurons in age-related macular degeneration. *Invest Ophthalmol Vis Sci*. 2001;42(3):795–803.
99. Lee EK, Yu HG. Ganglion cell–inner plexiform layer and peripapillary retinal nerve fiber layer thicknesses in age-related macular degeneration. *Invest Ophthalmol Vis Sci*. 2015;56(6):3976–3983.
100. Savastano MC, Minnella AM, Tamburrino A, Giovinco G, Ventre S, Falsini B. Differential vulnerability of retinal layers to early age-related macular degeneration: evidence by SD-OCT segmentation analysis. *Invest Ophthalmol Vis Sci*. 2014;55(1):560–566.
101. Lamin A, Oakley JD, Dubis AM, Russakoff DB, Sivaprasad S. Changes in volume of various retinal layers over time in early and intermediate age-related macular degeneration. *Eye (Lond)*. 2019;33(3):428–434.
102. Yenice E, Şengün A, Soyugelen Demirok G, Turaçli E. Ganglion cell complex thickness in nonexudative age-related macular degeneration. *Eye (Lond)*. 2015;29(8):1076–1080.
103. Gilbert CD, Wiesel TN. Receptive field dynamics in adult primary visual cortex. *Nature*. 1992;356(6365):150–152.
104. Baseler HA, Gouws A, Haak KV, et al. Large-scale remapping of visual cortex is absent in adult humans with macular degeneration. *Nat Neurosci*. 2011;14(5):649–657.
105. Owen WG. Spatio-temporal integration in the human peripheral retina. *Vision Res*. 1972;12(5):1011–1026.